SSRG International Journal of Electronics and Communication Engineering
ISSN: 2348-8549/ https://doi.org/10.14445/23488549/IJECE-V10I6P105

Volume 10 Issue 6, 35-51, June 2023

Original Article

Supervised Learning-Based Noise Detection to Improve the Performance of Filter-Based ECG Signal Denoising

Veerabomma Supraja[1,2*], Pasumarthy Nageswara Rao[3], Mahendra Nanjappa Giri Prasad[4]

[1]*Department of Electronics and Communication Engineering, Jawaharlal Nehru Technological University, Anantapur, Anantapuramu, Andhra Pradesh, India*
[2]*Ravindra College of Engineering for Women, Kurnool, Affiliated to Jawaharlal Nehru Technological University, Anantapur, Anantapuramu, India*
[3]*Department of Electronics and Communication Engineering, Vardhaman College of Engineering, Anantapuramu, Andhra Pradesh, India*
[4]*Department of Electronics and Communication Engineering, Jawaharlal Nehru Technological University, Anantapur College of Engineering, Anantapuramu, Andhra Pradesh, India*

[*]*Corresponding Author : suprajaece10@gmail.com*

Received: 28 March 2023 Revised: 22 May 2023 Accepted: 12 June 2023 Published: 30 June 2023

Abstract *- A significant purpose in detecting pervasive computing approaches is to improve the specificity and sensitivity of arrhythmia detection using electrocardiograms. Because ECG signals frequently propagate over distributed computer settings such as the medical Internet of things, noise is prevalent (medical IoT). In these distributed and widespread computing-aided methodologies, noisy electrocardiograms are common to false alarms. The fundamental goal of the machine learning-based arrhythmia detection algorithms discussed in this publication is to detect noise scope in electrocardiograms. The suggested approach determines whether or not the provided electrocardiograms are influenced by noise. In this regard, the approach takes advantage of the electrocardiogram's temporal and spectral characteristics. The performance of the suggested technique was evaluated using multifold cross-validation. In addition, a comparative study was performed comparing the average of peak Signal to Noise Ratio, respective standard deviation and filter sequence length obtained from filtering noise by FIR and IIR filters from raw ECG signals and the SLND-selected noisy ECG signals.*

Keywords *- Electro Cardiogram (ECG), Baseline Wandering (BA), Powerline Interference (PLI), Weiner Filter (WF), Fourier-transform (FT), FIR, IIR.*

1. Introduction

ECG is the commonly used cardiology test for assessing heart performance, wherein the electrical readings provide significant inputs [1]. The electrodes' essential function is detecting small electrical changes resulting from the facets of repolarization and depolarization, wherein the electrophysiological pattern for the heart muscles is assessed at each level of the heartbeat conditions [1]. Many distinct observations result in outcomes from the tests. For instance, there is potential scope for measuring heart rate consistency, size, and placement of the heart function conditions. Even the evaluations about the performance of any implanted devices like pacemakers or other such regulating medical devices, too, can be assessed.

The graph movements indicate the heart's function during the period wherein the medical devices are used to detect the heart rates by placing the device nodes over the skin's outer surfaces and the electrodes that are being observed. ECG (Electro Cardiogram) is the device used for garnering data as ECG signals constitute specific indicators as the common readings from the system, technically defined as Intervention Basic and Interference feed line.

Information garnered from the readings of ECG devices can be efficient for measuring the abnormalities in the heart rhythms [2, 3] and more categorically in assessing the fundamental readings to guide any significant and detailed tests to be carried out [4]. As discussed in [5], the ECGs can be very resourceful for detecting damage to specific portions based on the myocardium resulting from myocardial infractions [5]. The other important aspect is digitally collecting information and the ECG data, which will be resourceful for automatically handling the ECG signal analysis [6].

Routine electrical line readings and the baseline drift [7] are the two distinct factors that signify the actual condition of

the readings from a patient record for whom the ECG records are tested. The interference power line results from streams due to the inaccuracies like the improper placement of the electrodes, unhygienic electrodes, or any loose contact over the machinery.

The interference power line is usually 50 Hz. The basal movement results in the flexible impedance from electrode skin for the patient's response [8, 9]. Those two critical factors are vital in the clinical monitoring and ECG signal masks for patients' diagnoses. Despite the scope that applying a filter is feasible for reducing the noise power (stopband notch filter), it still does not suffice the requirement in handling the scale or frequency characteristics of the noise. Considering the constraints, the optimal signal focus on non-stationary processes remains the choice for handling noise reduction.

Conventional models were only successful to an extent. Specific models like the adaptive filtering procedures have been considered for cancelling the non-static interference. Filtration is when the signal's noise ratio is eliminated or mitigated to the optimal extent [10, 11]. The other significant aspects of the filtering process are smoothing and prediction. Numerous approaches were proposed for addressing enhancements to the process using ECG adaptive and other novel range of techniques used for filtering [12]. The adaptive filtering process is generally based on the cardinal model essential for managing signals without statistical signal characteristics.

One of the ECG process constraints is frequent interruption due to distinct noises and other disturbances. Earlier works have classified the interruptions [13-15] as BA (Baseline Wandering), PLI (Powerline Interference), and MA (Muscle Artifacts). Certain factors, like the subject movements of the respiratory activities, lead to BA, which manifests in slow wandering baselines resulting from facets like the body movements, which could be random.

ECGs constituting the impact of MAs have a critical issue of muscular contraction artifacts. PLIs lead by electrical power leakage or inappropriate equipment handling conditions significantly impact ECG amplitudes and an indistinct set of isoelectric baseline conditions. It is imperative to address such conditions of noises leading to disturbances, as the ECG signal analysis interpretation might lead to misled or inaccurate insights for diagnosis.

Introduction to the ECG and numerous other models are covered in section 1 of this document. The related work in ECG for noise detection has been investigated in section 2, and a variety of literature has been studied and presented. Materials and procedures are covered in Section 3. In an experimental study found in Section 4, the proposed and current models' performance is compared using several indicators. After the references, Section 5 concludes.

2. Related Work

A signal generally constitutes a specific noise factor resulting from distinct internal and external surrounding aspects. In biomedical solutions, reducing such noises to a greater extent is highly important to mitigate the interferences and increase detection accuracy for better diagnosis conditions. Numerous studies have highlighted the conditions leading to noise as muscle or motion-related interferences, baseline wander conditions, etc., which overlap the signal conditions [16].

The filtering process can be essential to attain noise-free signals. A correct method for filtering has to be handled effectively, as any gaps in the process might lead to an incorrect filtering model, which might distort the other signal conditions [17].

From the literature review, it is evident that many studies from the past have focused on addressing noise elimination in ECG signals. In [18], the authors have proposed the solution as WF (Weiner Filter) designed for a stationary signal and to minimize the error rate. However, the non-stationary behaviour tendency of the ECG system makes the noise elimination conditions an ineffective solution. The other model discussed for the purpose is [19] and [20], wherein the methods focus on cancelling the signal noises like EMG, PLI, BW, and MA. However, in the further model discussed in [21], such effectiveness's accuracy rate is increased. Despite all such efforts, there is still considerable scope for denoise of non-cardiac ECG noises.

The methods such as Wavelet transforms, as discussed in [22-24], are known for their effectiveness in denoise of ECG signals. Such noise reduction is executed in the frequency domain to achieve superior performance and determine the best threshold.

In [25], the efforts focus on the combination of DWT and NLM methods, in which the pattern of signal decomposition is executed at two distinct levels. The variances of co-efficiency for the first and second levels were observed in the ranges of higher frequencies and low-frequency noise conditions that rely on the NLM method for address. The NLM methods have the approximation of co-efficiency in the second-level conditions.

In [26], the EMD method constituting ASMF (Adaptive Switching Mean Filter) has been discussed. The process adopted in the system uses three IMFs resulting from the decomposition process to eliminate the high-frequency noises and the reconstruction process. Signals are processed based on the ASMF method in terms of essential

enhancements. In [27], the method of EMD is known for combination with DWT and VMD in combination with DWT.

In [22], the authors have discussed the prospect of an NLM filtering model, which can remove noises from the images. NLM is a parametric model that requires numerous parameters to be set. The value of such parameters needs more accurate analysis, as it directly impacts the results. Many of the earlier methods have attempted to de-noise ECG signals based on a distinct set of solutions discussed in [28-32] for wavelet transformation and adaptive filtering technique discussed, weighted average models proposed in [33-37] EMD, and Independent Component Analysis [38]. In [39], authors have iterated on how many existing models have distinct noise-removal limitations. The adaptive filters proposed in [40] can lead to the signed regression algorithm filters and stabilized least-mean square conditions. However, there are complexities in attaining noise-signal references from a conventional system of ECG signal readings. New solutions that have focused on ECG-related studies have focused on novel solutions. In a comparative study, the researchers have focused on a huge scale of data collection-oriented noise reduction [41, 42]. Tracking the data from ECG systems for monitoring the patients from ICU (intensive care units) was discussed in [43, 44]. It is imperative for more digital storage of readings for comparative analysis; there is a need for more effective solutions to address the noise issue in ECG readings. Numerous other studies focused on handling distinct models, as discussed in [45]. The EMD model constituting NLM is adapted to eliminate white and colour Gaussian noise conditions. The contemporary model "Denoising of Electrocardiogram (ECG) signal by using empirical mode decomposition (EMD) with non-local mean (NLM) technique (EMD+NLM)" [45].

3. Methods and Materials

The methods and associated materials used in the proposed model have been explored in this section. The methods used to fulfil the objectives of the learning phase, such as the method of selecting features and optimizing those features to reduce the process complexity. The classifier trained by the corresponding optimal features and classifies the noise from the given electrocardiogram input is detailed in the following subsections. Figure 1 represents the SLND block diagram.

3.1. Features

The temporal features of the electrocardiogram signal, such as energy and zero-rate crossing, shall be considered to explore the signal's physical structure. The spectral-related feature can be obtained by morphing the signal of the time domain to the frequency domain. This phase of converting a signal from the time domain to the frequency domain can be done using Fourier transformation [46]. Further, the frequency domain's resultant signal shall be used as input to derive spectral features such as frequency and its components, density, flux, roll-off, and the centroid of the corresponding spectrum. However, concerning the electrocardiograms, random variables to analyze noise spectrum evince complexity compared to electrocardiogram signals. A random spectrum with no information shall be considered to determine the spectral features from the signals' static noise [47]. The static noise does not have any special or unexpected occurrences. Hence, a significant variance can appear between static noise signals and signals of electrocardiograms. The Fourier transformation decomposes the electrocardiogram signal, which results in the spectral structure, diversified frequencies, and magnitudes. The prediction of noise is more robust if temporal features such as MCC (Max-coefficient-correlation), energy, index, and zero or null crossing rate (NCR or ZCR) are considered along with spectral-domain features GTCC (Gammatone-cepstral-coefficients) and MFCC (Mel-Frequency-Cepstral-Coefficients).

3.2. Kolmogorov-Smirnov Test (KS Test)

The KS-test statistics show differences between a distribution and a sample distribution. Report it as the disparity between two samples drawn randomly from the same or different sizes of the experimental distribution. To demonstrate how unlike the distributions of the two datasets are, the KS-test [48] employed a distance measure known as the KS-test (for the "Kolmogorov-Smirnov test"). Other distance measures automatically determine the degree of diversity in a distribution, but this metric does not require prior knowledge of the data distribution. The algorithmic procedure for conducting a KS test is also outlined below:

$ks\_test(v_1, v_2)$ Begin //Two vectors are used as input.

A primary function of the procedure is to foretell the sequential accumulation of vectors. Additionally, the cumulative ratios are shown as vectors matching the criteria.

$pr = 0$	// It has been foreseen that the summation of each vector's component will provide a specific ratio.
$\forall \{e_i \exists e_i \in v_j\}_{i=1}^{\lvert v_j \rvert} begin$	Every component of a vector is taken in this iteration.
$pr = \frac{e_i}{Ag(v_j)} + pr$	In this illustration, the accumulated ratio of the predecessor element is shown in reiteration.
$CR_{v_j} \leftarrow pr$	refers to the sum of the values shown in the vector,
end	the set CR_{v_j} consists of average proportions of all components present in vector v_j

Later, the values arising from the absolute cumulative ratios of distances with the same vector index will be identified.

$$\max_{\substack{\forall \\ i=1}}(|CR_{v_a}|,|CR_{v_b}|)\left\{\begin{matrix} c_i(v_a), c_i(v_b) \exists \\ c_i(v_a) \in CR_{v_a} \wedge c_i(v_b) \in CR_{v_b} \end{matrix}\right\}$$ //values existed for each index

Begin

$$\mathrm{AD}_{\mathrm{CR}_{\mathrm{v_a}} \leftrightarrow \mathrm{CR}_{\mathrm{v_b}}} \leftarrow \mathrm{abs}(\mathrm{c_i}(\mathrm{v_a}) - \mathrm{c_i}(\mathrm{v_b}))$$ // represents the absolute distance between cumulative ratios expressed as sets.

End

Identify d-stat, which would be the highest value that is existed in $AD_{CR_{v_a} \leftrightarrow CR_{v_b}}$

The d-critic aimed at the KS table has been identified for $Ag(v_a), Ag(v_b)$ provided for the degree of threshold probability $p\tau$

If the d-stat depicted is greater than the d-critic presented, return 0//2 vectors are not distinct.
Else return 1 //two vectors are distinct
End

Table 1. Description of the formulas and acronyms

Medical IoT	**Medical Internet of Things**
ECG	Electro Cardiogram
BW	Baseline Wandering
PLI	Powerline Interference
WF	Weiner Filter
FT	Fourier-Transform
ASMF	Adaptive Switching Mean Filter
EMD	Empirical Mode Decomposition
NLM	Non-Local Mean
SLND	Electrocardiogram Noise Detection and Quality Estimation
ICU	Intensive Care Units
MCC	Max-Coefficient-Correlation
MFCC	Mel-Frequency-Cepstral-Coefficients
v_a, v_b	Vectors
$Ag(v_a), Ag(v_b)$	Aggregation
CR_{v_a}, CR_{v_b}	Cumulative Ratios
e_i	Element
pr	Previous Element in Reiteration
AD	The Absolute Distance
$p\tau$	Threshold Probability
WCs	Weak Classifiers
D_t	Distribution
$h_t: X \rightarrow \{-1, +1\}$	Hypothesis
$PandN$	Positive and Negative
tf_i	Temporal-Feature
SF	Spectral Feature
nG	N-grams
r_j	Record

3.3. The Classifier

Adaboost is a collective learning approach optimized for boosting binary classifiers' accuracy. As a bonus, Adaboost employs an iterative approach to learn from the mistakes of weak classifiers and then correct those mistakes with more robust methods.

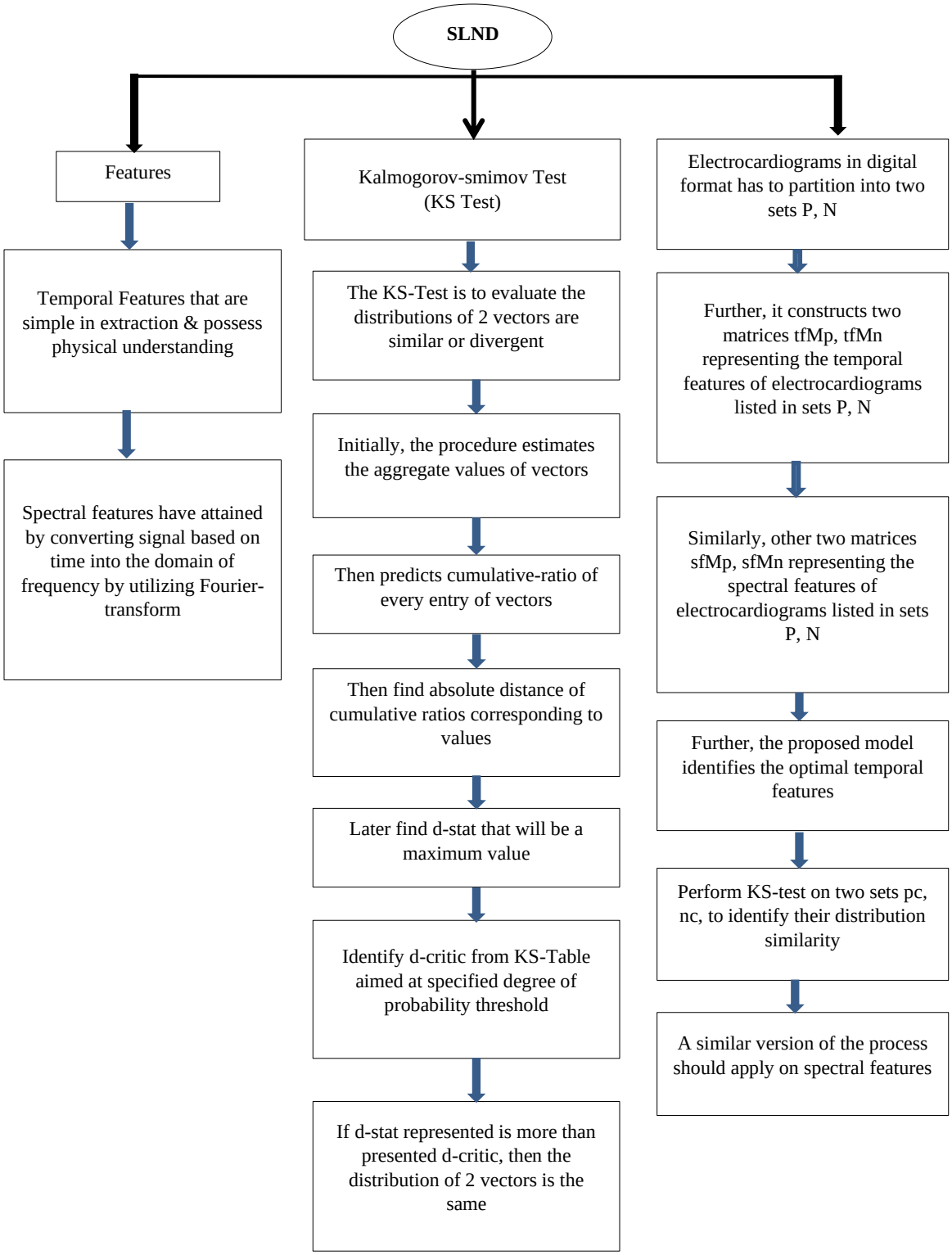

Fig. 1 SLND is shown as a block diagram

Adaboost has evolved into the adaptive reinforcement method [49]. This classifier was made to include weak classifiers (WCs) or those that use a branching Boolean formula. Each weak classifier creates a false or true condition based on the input data. The other WCs will split false positives and negatives (the negatives). This procedure is repeated until all members of the WC are involved in the negotiations necessary to finish the challenge. The final results from the ranking method should include all information collected from these low-quality classifiers [50]. In this article, WC refers to the ideal qualities compatible with the binary classification, which is the focus of the proposed model. The process of sorting is an iterative one. Weak classifiers commonly use reinforcement learning, in which the centre region that did not correctly categorize repeats the previous classifier. Here the Week Classifier, which is used for each iteration, shall be referred to by the rating weight. With the completion of iterative WC calls, WC-scored records shall be completely streamlined. Regarding the predicted method, Adaboost uses each WC, indicating a specific n-gram number to rank the accuracy. Besides, the WC classification results would streamline discovering the polarity of specific records against the proposed method [51]. A WC and the like would be involved for each feature class, and each class of the appropriate features would learn about the noisy and qualified electrocardiograms. The mathematical model of the Adaboost classification is described in the following. Eq 1

$$(x_1, y_1), \ldots\ldots, (x_m, y_m), \text{here } x_i \in X, y_i \in \{-1, +1\} \quad (1)$$

Initialize: $D_1(i) = 1/m$for $D_1(i) = 1/m \;\; i = 1, \ldots\ldots, m$

For $t = 1, \ldots., T$

- Use distribution to instruct hesitant learners D_t
- Get a weak hypothesis $h_t: X \to \{-1, +1\}$
- Goal: Choose h_t with a small weighted error

$$\varepsilon_t = P_{r_{i\sim D_t}}[h_t(x_i) \neq y_i] \quad (2)$$

- Choose $\alpha_t = \frac{1}{2} In\left(\frac{1-\varepsilon_t}{\varepsilon_t}\right)$
- Update, for $i = 1, \ldots\ldots, m$

$$D_{t+1}(i) = \frac{D_t(i)\exp(-\alpha_t y_i h_t(x_i))}{Z_t} \quad (3)$$

Where the normalizing factor is Z_t (chosen so that D_{t+1} will be a distribution)

The conclusion is given:

$$H(x) = Sign(\sum_{t=1}^{T} \alpha_t h_t(x)) \quad (4)$$

3.4. Electrocardiogram Noise Detection and Quality Estimation

Separate the supplied collection of electrocardiograms into two groups, P and N, with P representing the positive recordings (where the digitally defined signal is a valid ECG) and N representing the negative recordings (refers to the noisy ECG).

Specifically, the proposed model generates two tables, $tfMp$ and $tfMn$, that list the temporal properties of electrocardiograms according to the categories P and N. The spectrum properties of the electrocardiograms are similarly shown in Tables sfMp and sfMn. In the suggested model, the ideal temporal properties are determined by the following equation:

$$\forall_{|tfMp|}^{i=1} \{pc_i, nc_i \exists pc_i \in tfMp \wedge nc_i \in tfMn\} \quad (5)$$

// Iterates until all the columns of both tables are processed, considering the column$pc_i$from the table $tfMp$ and the column $nc_i$from the table $tfMn$ as inputs to KS-test

The function $ks - test(pc_i, nc_i)$ invokes the vectors pc_i, nc_ias input parameters, which predicts the diversity between these two vectors. If diversity is found between these vectors, then the temporal feature tf_i representing these vectors shall be considered optimal. If not (no diversity found), then the feature tf_i is suboptimal. Hence discard the corresponding vectors pc_i, nc_i from the respective sets $tfMp$ and $tfMn$.

After the conclusion of the iterations in equation 5, the tables $tfMp, tfMn$ retain values for optimal features. A comparable form of the process shall apply to the spectral feature tables $sfMp, sfMn$, which results in the optimal spectral features. As discussed in the next section, the several phases determine the best n-gram characteristics, including both labels.

3.5. Discovering N-Gram Features

The features representing the columns of the resultant sets $tfMp, tfMnsfMp, sfMn$ as input, it is utilized to find all possible distinct subsets, denoted by n-gram features in subsequent descriptions. The following discussion delves into the mathematical paradigm for discovering n-grams with dynamic sizes.

$n-gram\_features(aL)$ Begin	
$nGr \leftarrow aL$	The standard set of 1-grams is aL. The qualities indicated inside the set aL will thus be added to the set of n-grams, nG.
$tnG \leftarrow nGr$	Set tnG is a clone as Set nGr.
while($\lvert tnG\rvert > 0$)Begin	While not being empty, set tnG
$\overset{i=1}{\underset{\lvert tnG\rvert}{\forall}} \{ng_i \exists ng_i \in tnG\}$ Begin	For every n-gram ng_i in the set, tnG
$\overset{\mathrm{j}=1}{\underset{\lvert \mathrm{tnG}\rvert}{\forall}} \{\mathrm{ng_j} \exists \mathrm{ng_j} \in \mathrm{tnG} \wedge \mathrm{i} \neq \mathrm{j}\}$ Begin	For every tnG set n-gram $\mathrm{ng_j}$ Which isn't equal to n-gram ng_i
$ng \leftarrow \{ng_i \cup ng_j\}$	Two n-grams ng_i, ng_j combine to form the new n-gram ng, which represents
$if(ng \notin nGr) nGr \leftarrow ng$	Add n-gram ng to the set nGr with n-grams if it is absent from the set nGr of n-grams.
End	// the loop of $\overset{j=1}{\underset{\lvert tnG\rvert}{\forall}} \{ng_j \exists ng_j \in tnG \wedge i \neq j\}$
End	// the loop of $\overset{i=1}{\underset{\lvert tnG\rvert}{\forall}} \{ng_i \exists ng_i \in tnG\}$
$if(\lvert nGr\rvert > \lvert tnG\rvert)$ Begin	If set nGr size $\lvert nGr\rvert$ is larger than $\lvert tnG\rvert$ size,
$tnG \backslash tnG$	Empty the set N14tnG
$tnG \leftarrow nGr$	Add each of the set nGr n-grams towards the empty set tnG.
End	condition N15 if($\lvert nGr\rvert > \lvert tnG\rvert$)
else if ($\lvert nGr\rvert \equiv \lvert tnG) tnG \backslash tnG$	Empty every set tnG if both sets nGr, tnG have the same size.
End	// the loop while($\lvert tnG\rvert > 0$)

The resulting set nGr comprises all potential subsets of the set'saL characteristics (column labels). The suggested technique then determines the n-gram attribute values as well as their confidence in both sets tD_+, tD_-, as shown below.

$\overset{i=1}{\underset{\lvert nGr\rvert}{\forall}} \{ng_i \exists ng_i \in nGr\}$ Begin	// For each n-gram, $\mathrm{ng_i}$ characteristic of the set, and nGr
$fv(ng_i)$	// is indeed an empty set that includes both negative as well as positive labels together with unique n-gram attribute values for said n-gram feature $\mathrm{ng_i}$.
$\overset{j=1}{\underset{\lvert tD_+\rvert}{\forall}} \{r_j \exists r_j \in tD_+\}$ Begin	// For every r_j record in the tD_+ set
$fv(ng_i) \leftarrow \{v(ng_i) \exists v(ng_i) \subseteq r_j \wedge v(ng_i) \notin fv(ng_i)\}$	Values $\mathrm{v(ng_i)}$ belong to a subset of the record $\mathrm{r_j}$ of the positive label and do not exist in the set $\mathrm{fv(ng_i)}$ of the n-gram feature $\mathrm{ng_i}$

End // of the loop $\overset{j=1}{\underset{|tD_+|}{\forall}} \{r_j \exists r_j \in tD_+\}$

$\overset{j=1}{\underset{|tD_-|}{\forall}} \{r_j \exists r_j \in tD_-\}$ Begin // for every record r_j in the set tD_- with negative records

$$fv(ng_i) \leftarrow \{v(ng_i) \exists v(ng_i) \subseteq r_j \wedge v(ng_i) \notin fv(ng_i)\}$$

$v(ng_i)$ subset of record values $r_j$of the negative label and do not exist in the set $fv(ng_i)$ of the n-gram feature ng_i

End // the loop $\overset{j=1}{\underset{|tD_-|}{\forall}} \{r_j \exists r_j \in tD_-\}$

End // of the loop $\overset{i=1}{\underset{|nGr|}{\forall}} \{ng_i \exists ng_i \in nGr\}$

Identifying both negative and positive confidence levels of every n-gram attribute values

$\overset{i=1}{\underset{|nGr|}{\forall}} \{ng_i \exists ng_i \in nGr\}$ Begin // for every n-gram, ng_iset feature nGr

$\overset{j=1}{\underset{|fv(ng_i)|}{\forall}} \{v_j \exists v_j \in fv(ng_i)\}$ The individual n-gram feature values v_j and ng_i

$$pc_+ \leftarrow \frac{1}{|tD_+|}\left(\sum_{k=1}^{|tD_+|}\{1 \exists v_j \subseteq r_k)\}\right)$$

Increase positive confidence in the n-gram feature valuev_j

$$pc_- \leftarrow \frac{1}{|tD_-|}\left(\sum_{k=1}^{|tD_-|}\{1 \exists v_j \subseteq r_k)\}\right)$$

Move negative confidence of n-gram feature valuev_j

End //of the loop $\overset{j=1}{\underset{|fv(ng_i)|}{\forall}} \{v_j \exists v_j \in fv(ng_i)\}$

End // of the loop $\overset{i=1}{\underset{|nGr|}{\forall}} \{ng_i \exists ng_i \in nGr\}$

The resultant n-gram features of both temporal and spectral formats shall be used to train the classifier that classifies whether the given electrocardiogram is noisy.

4. Experimental Study

The experimental study intended to exhibit the significance of the proposed method SLND. The experiments have carried cross-validation of the proposed method SLND and contemporary model "Denoising of Electrocardiogram (ECG) signal by using empirical mode decomposition (EMD) with a non-local mean (NLM) technique (EMD+NLM)" [45] using benchmark dataset MIT-BIH [52]. The resultant cross-validation metric values of both methods have compared and scaled the performance of the proposed model SLND. The overall records constituted in the adopted corpus of electrocardiograms are 14423 (7802: qualified electrocardiograms and 6621: noisy electrocardiograms)

Tenfold cross-validation has been performed on the dataset with qualified and noisy electrocardiograms.

Concerning tenfold cross-validation, the dataset of both labels was partitioned into ten equal shares. On each cross-validation fold, one share of the dataset has been used for testing, and the remaining nine shares have been used for training.

4.1. The Performance Analysis

4.1.1. Supervised Learning-Based Noise Detection

The cross-validation metric values have been compared and analyzed the performance in Table 2. The results obtained for cross-validation metrics report the performance significance of the proposed method SLND over the contemporary method EMD+NLM. Metric-level details have been explored in the following description.

The cross-validation metric precision refers to the positive predictive value obtained from both methods through cross-validation: 0.88640.0098 (89%) and 0.861580.014976502 (86.5%), respectively, order of SLND and EMD+NLM. The details of precision observed from each fold of the cross-validation are figured out in Figure 2. The values obtained for metric precision report the significance of the SLND with minimal deviation compared to the contemporary model EMD+NLM.

The True Negative Rate that refers to specificity observed for SLND and EMD+NLM methods are 0.9397±0.0061 (94%, and 0.9261±0.0095 (93%) from tenfold cross-validation. The specificity observed from each cross-validation fold has been briefed in Figure 3. The values obtained for metric specificity report the significance of the SLND with minimal deviation compared to the contemporary model EMD+NLM.

The actual positive rate also refers to sensitivity observed from cross-validation performed on both methods SLND, EMD+NLM are 0.9532±0.00546 (95%) and 0.9290±0.0086 (93%) in respective order. The details of the fold level sensitivity have been figured out in Figure 4. The values obtained for metric sensitivity report the significance of the SLND with better performance compared to the contemporary model EMD+NLM.

Table 2. Values obtained for cross-validation metrics from SLND and EMD+NLM methods

FOLD ID#	1	2	3	4	5	6	7	8	9	10
PRECISION										
SLND	0.9062	0.8743	0.8812	0.8853	0.9023	0.884	0.8756	0.886	0.8827	0.8868
EMD+NLM	0.8406	0.8364	0.8676	0.8508	0.8553	0.8792	0.8839	0.8729	0.8612	0.8679
SENSITIVITY										
SLND	0.9405	0.9535	0.9599	0.9503	0.9474	0.9579	0.9563	0.9567	0.9553	0.9544
EMD+NLM	0.9194	0.9376	0.9159	0.928	0.9472	0.9338	0.9271	0.9239	0.9306	0.9263
SPECIFICITY										
SLND	0.9522	0.9321	0.9358	0.9395	0.9495	0.9381	0.9332	0.9391	0.9373	0.9398
EMD+NLM	0.9137	0.9092	0.9307	0.9199	0.921	0.9365	0.9398	0.9338	0.9258	0.9304
ACCURACY										
SLND	0.9483	0.9394	0.9441	0.9428	0.9487	0.9445	0.9407	0.9449	0.9432	0.9445
EMD+NLM	0.9157	0.9186	0.9258	0.9225	0.9297	0.9356	0.9356	0.9305	0.9275	0.9292
F-MEASURE										
SLND	0.9286	0.9023	0.9077	0.9116	0.9253	0.9102	0.9035	0.9118	0.9092	0.9125
EMD+NLM	0.8756	0.8713	0.898	0.884	0.8869	0.9069	0.911	0.9023	0.8923	0.8981
MATHEWS CORRELATION COEFFICIENT										
SLND	0.8847	0.8681	0.8783	0.8743	0.8862	0.8788	0.871	0.8795	0.8759	0.8783
EMD+NLM	0.8158	0.8248	0.8354	0.8306	0.8479	0.8576	0.8568	0.8461	0.841	0.8439

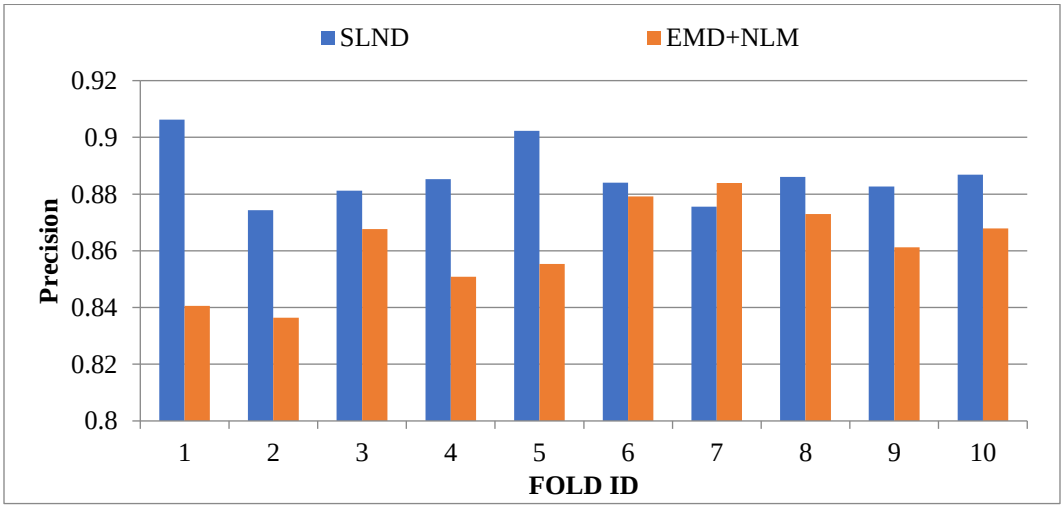

Fig. 2 The positive predictive values observed from cross-validation

The cross-validation metric "prediction accuracy" denotes the ratio of correctly labelled records against the total number of records. The overall prediction accuracy observed for SLND and EMD+NLM is 0.9441±0.0028 (95%) and 0.92707±0.0063 (93%). The detailed statistics of accuracy obtained from tenfold cross-validation have been explored in Figure 5.

The values obtained for metric accuracy report the significance of the SLND with better performance compared to the contemporary model EMD+NLM. The cross-validation metric "F-measure" has been measured over the proposed and contemporary models among ten folds, as shown in Figure 6. In respective order, the average f-measure depicted for SLND and EMD+NLM are 0.91±0.008 (91%) and 0.8926±0.012 (89%).

The detailed statistics of F-measure obtained from tenfold cross-validation have been explored in Figure 6. The values obtained for metric f-measure exhibit the significance of the SLND with better performance when compared to the contemporary model EMD+NLM.

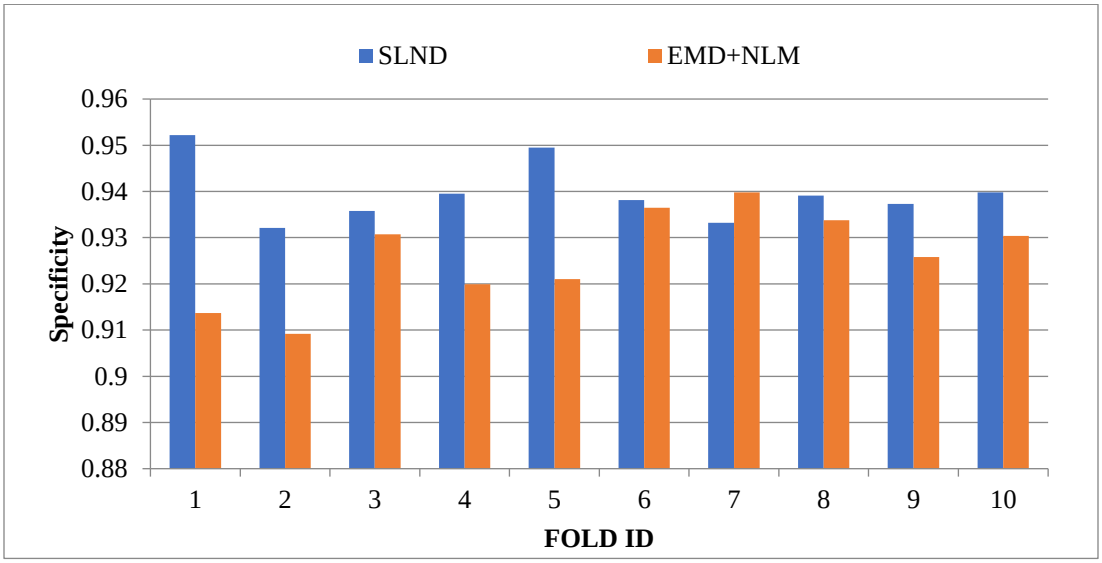

Fig. 3 The true negative rate obtained from cross-validation

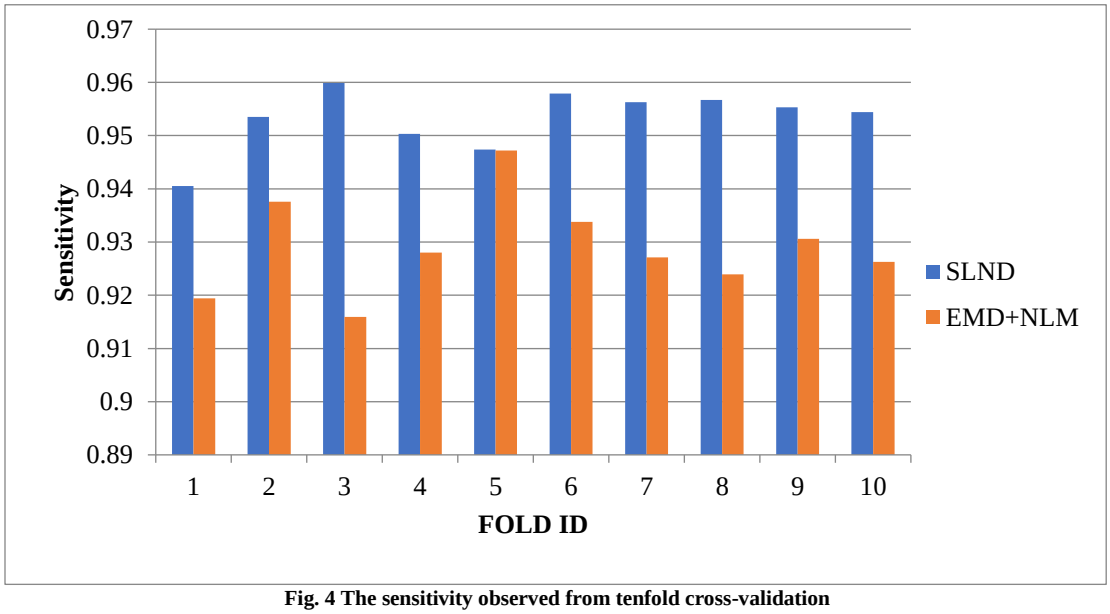

Fig. 4 The sensitivity observed from tenfold cross-validation

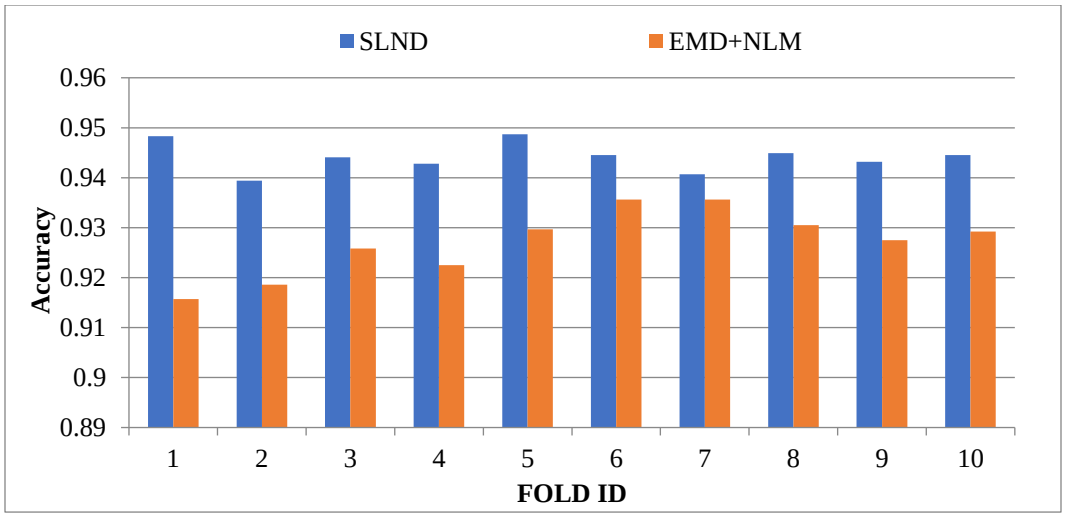

Fig. 5 Accuracy obtained from tenfold cross-validation

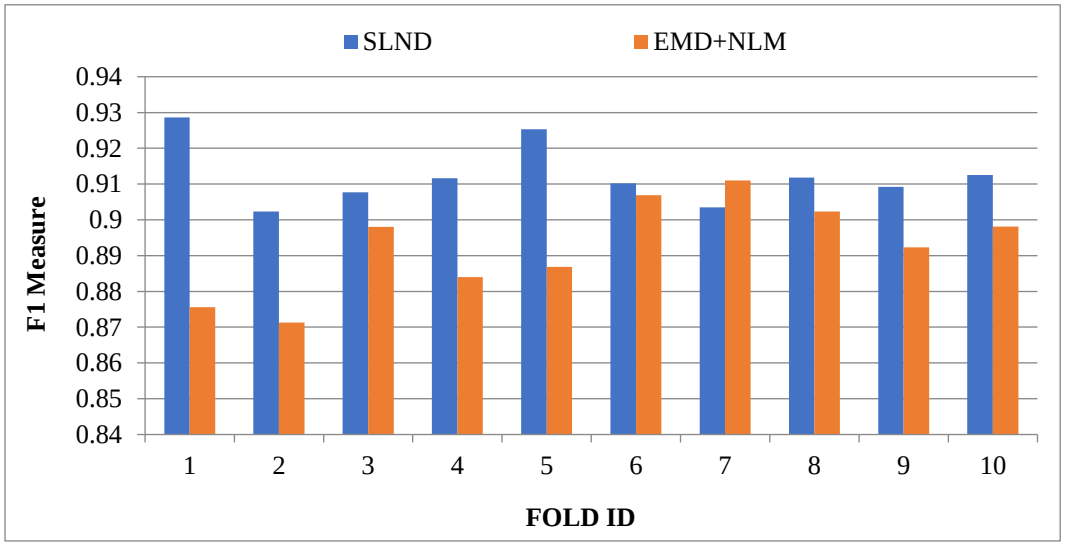

Fig. 6 The f-measure observations from tenfold cross-validation

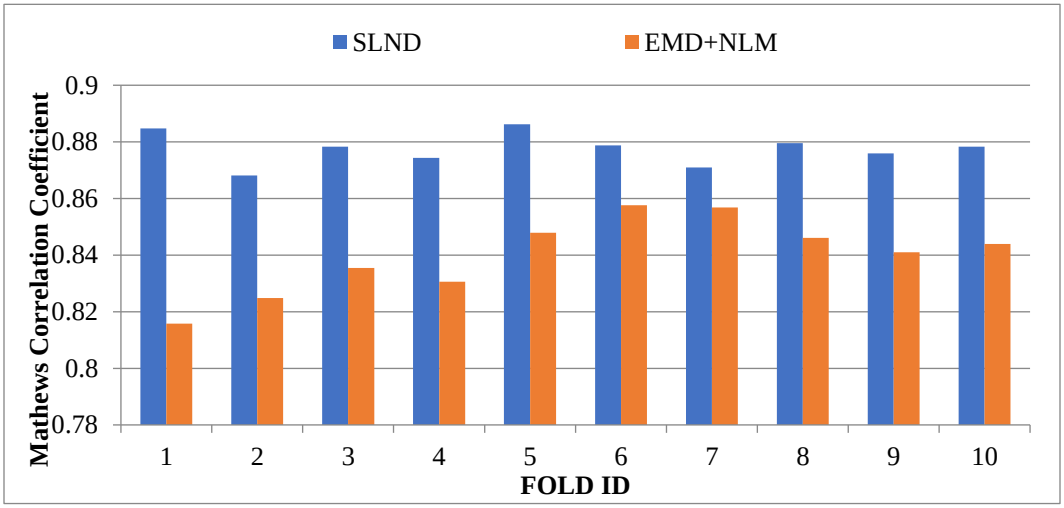

Fig. 7 The Mathews Correlation Coefficient (MCC) observed from the tenfold cross-validation

The cross-validation metric MCC has been measured over the proposed and contemporary models among ten folds, as shown in Figure 7. The MCC observed for SLND and EMD+NLM are 0.8780.005 (89%) and 0.840.013 (84%) in the respective order. The detailed statistics of MCC obtained from tenfold cross-validation have been explored in Figure 7. The values obtained for metric MCC exhibit the significance of the SLND with better performance when compared to the contemporary model EMD+NLM.

4.1.2. Filter Sequence-Based Denoising of Raw Signal and SLND Selected Signal

Below, we detail the methodology used in this investigation and provide a high-level summary.

ECG Data Loading**:** This research measures SNR at different filter orders. We used the data corpus "MIT-BIH ECG-ID", which comprises 500 Hz ECG data [53-55]. Eight raw and processed databases are used. Denoising is implemented in Python. This study employed an 8-GB Intel Core i5 Windows machine. Per the data set, processing takes 1 minute.

Choose a low-order pass filter**:** FIR and IIR filter designs are used in this research. Each output sample is computed by weighing and adding the input samples. Output values and input points are used in IIR filters. The term "recursive" refers to the fact that these filters recur [56]. The Python and Scipy library is used to apply these filters [57]. The filter level is raised by one after each repetition, up to 100.

ECG Signal Filtering**:** The peak power of the electrocardiogram signal occurs between 0.5 and 45 Hz, with a frequency range from 0.05 to 150 Hz. There is a 0.67–5 Hz P wave, a 10–50 Hz QRS complex, and a 1–7 Hz T wave. There is interference in some frequency bands. ECG artefacts and noise levels [58-60] include muscle noise from 5 to 50 Hz, respiratory noise from 0.12 to 0.5 Hz, and electrical sounds from 50 to 60 Hz. Filtering the heart's electrical activity can be used for diagnosis or monitoring. Diagnosis occurs between 0.05 and 150 Hz [61]. 0.5 - 40 Hz [62] is the sampling rate of the following series. Eight groups of raw ECG signals are filtered, all at 500 Hz, with 10,000 samples.

According to the data, the Butterworth low passband filter's Passband corners frequency (Wp) is 40 Hz. In comparison, the Stopband corners frequency (Ws) is 60 Hz, the Passband ripple (Rp) is 0.1 dB, and the Stopband attenuation (Rs) is 30 dB.

The SNR response of filter designs in diagnostic and monitoring ECG frequency ranges was investigated in this work. Constant filter parameters are used to compare filter designs. The monitoring Frequency Range (40 Hz Passband, 60 Hz Stopband) and Diagnostic Frequency Range are the filter settings (Passband corners frequency at 150 Hz, Stopband corners frequency at 160 Hz). Evaluate SNR: The signal-to-noise ratio (SNR) is stated in decibels and is the ratio of signal power (insightful data) to noise power (unsolicited signal) Eq 6, Eq 7.

Table 3. Comparative study of peak SNR observed from diversified FIR filters during continuous monitoring of raw as well as SLND selected signals

FIR FILTER'S PEAK SNR						
Filter	**Mean of the Peak SNR (dB)**		**SD**		**Respective Filter Sequence**	
	Raw Signal	**SLND Signal**	**Raw Signal**	**SLND Signal**	**Raw Signal**	**SLND Signal**
Kaiser Window	6.0367	8.0367	1.3704	0.7798	25	17
Hanning Window	5.2224	7.2214	1.0839	0.6813	4	2
Maximally Flat	4.5363	6.5362	1.3307	0.8013	17	10
Constrained Least Square	4.8134	5.8133	1.3383	0.7013	24	14
Rectangular Window	6.1661	8.165	1.3726	0.5751	25	18
Hamming Window	5.3503	7.3494	1.0671	0.7051	3	1
Equiripple	8.0792	10.0789	1.3203	0.8059	8	5
Least Square	6.3361	8.3348	1.3204	0.8223	10	6
Bartlett Window	5.2216	7.2214	1.0831	0.7371	4	2
Blackman Window	5.2221	7.2213	1.0831	0.8142	4	2

Table 4. Comparative study of peak SNR of raw and SLND selected signals observed from diversified IIR filters during continuous monitoring of raw as well as SLND selected signals

IIR FILTER'S PEAK SNR						
Filter	**Mean of the Peak SNR (dB)**		**SD**		**Respective Filter Sequence**	
	Raw Signal	**SLND Signal**	**Raw Signal**	**SLND Signal**	**Raw Signal**	**SLND Signal**
Chebyshev type II	4.5514	5.3859	1.3266	0.6102	11-15	8-11
Butterworth	4.7234	5.5585	1.2326	0.8597	3-5	1-3
Chebyshev type I	5.0908	5.9333	1.1075	0.9191	3-6	1-4
Elliptic	5.0908	5.9311	1.1076	0.8252	2-5	1-3

Table 5. Comparative study of peak SNR observed from diversified FIR filters during diagnosis mode of raw as well as SLND selected signals

FIR FILTER'S PEAK SNR						
Filter	**Mean of the Peak SNR (dB)**		**SD**		**Respective Filter Sequence**	
	Raw signal	**SLND Signal**	**Raw Signal**	**SLND Signal**	**Raw Signal**	**SLND Signal**
Kaiser Window	6.284	7.2899	0.9326	0.7925	7	6
Bartlett Window	5.5039	6.385	1.0315	0.8766	9	7
Rectangular Window	6.368	7.3242	0.9248	0.7578	7	5
Constrained Least Square	5.846	6.8993	1.0602	0.8791	5	4
Equiripple	11.6343	13.3797	1.1167	0.9491	4	3
Maximally Flat	5.4553	6.5477	1.0487	0.8491	15	12
Hamming Window	5.4718	6.3484	1.0425	0.8332	13	10
Least Square	7.4526	8.6454	1.104	0.9161	4	3
Hanning Window	5.4744	6.2961	1.0382	0.8405	11	9
Blackman Window	5.4561	6.5483	1.0844	0.889	4	3

Table 6. Comparative study of peak SNR observed from diversified IIR filters during diagnosis mode of raw as well as SLND selected signals

IIR FILTER'S PEAK SNR						
Filter	**Mean of the Peak SNR (dB)**		**SD**		**Respective Filter Sequence**	
	Raw Signal	**SLND Signal**	**Raw Signal**	**SLND Signal**	**Raw Signal**	**SLND Signal**
Chebyshev type II	5.4321	6.4104	1.0466	0.8374	5-11	3-10
Elliptic	5.4175	6.2849	1.0969	0.8999	1-3	1
Chebyshev type I	5.4617	6.2821	1.0514	0.8943	1-4	2
Butterworth	5.4562	6.4388	1.0471	0.8591	2-5	1-3

$$\mathrm{SNR} = \frac{\mathrm{P_{signal}}}{\mathrm{P_{noise}}} = \left[\frac{\mathrm{A_{signal}}}{\mathrm{A_{noise}}}\right]^2 \quad (6)$$

$$\mathrm{SNR_{dB}} = 10\log_{10}(\mathrm{SNR}) \quad (7)$$

For each portion of the signal, several filters are successfully compared. The difference between the raw and processed signals is used to derive the random noise. Provided Electrocardiogram signal − Provided Filtered Signal = interference. Evaluating the SNR of different filtering models is now feasible since the denominator, i.e., the random noise, is consistent throughout all filtration methods.

Recurrent the process to maximum 100th filter in sequence: The method is recurrent for all filters in the sequence of maximum 100th filter after SNR has been assessed for the lowest feasible ordered filter. As a result, a link between SNR and filter order is discovered.

Find the peak SNR for a particular filter and the appropriate Filter Sequence: SNR results for all sequences of filters up to 100 are retained in an array. The array values are studied to identify SNR transition with filter order. Peak SNR solution is achieved at the filter sequence where SNR changes through lesser than 10-2 units.

Remaining Process Filters: The abovementioned steps are recurrent for all preferred filters, SNR, and filter sequence, and peak SNR is procured in diagnosis mode.

Performance of the Low Pass Filter During Continuous Monitoring of Raw and SLND Selected Signals

Tables 3 and 4 show the average peak SNR diversified sets of electrocardiogram signals and the filtration sequence length.

Performance of the low Pass Filter During Diagnosis Mode of Raw and SLND Selected Signals

Tables 5 and 6 show the average peak SNR diversified sets of electrocardiogram signals and the filtration sequence length.

5. Conclusion

This research provides a different technique for classifying supplied input electrocardiograms as qualified or noisy, reducing false alarms in machine learning-based arrhythmia diagnosis. The noise localization has been enhanced using a classification procedure that learns from the best temporal and spectral characteristics chosen using a KS-Test distribution diversity measure.

The classification procedure was performed using the Adaboost approach, which was trained using the chosen optimum features. The suggested technique achieves high accuracy in distinguishing between qualified and noisy electrocardiograms. The suggested method's performance was scaled using multifold cross-validation and empirical filtration by a sequence of IIR and FIR filters applied on both raw signals as noisy signals detected by the SLND.

The approach, however, is confined to determining the noise scope in electrocardiograms. Soft-computing approaches will be used in future studies to eliminate noise from electrocardiograms. The other potential research component will employ wavelet parameters to identify weak noise signals in electrocardiograms.

References

[1] A. Kumar, "ECG-Simplified, *LifeHugger*, 2010. [Google Scholar]

[2] Robert O. Bonow et al., *Braunwald's Heart Disease: A Textbook of Cardiovascular Medicine*, Elsevier Saunders, vol. 2, 9th Ed., 2021. [Google Scholar] [Publisher Link]

[3] Jimmy Ming-Tai Wu et al., "A Deep Neural Network Electrocardiogram Analysis Framework for Left Ventricular Hypertrophy Prediction," *Journal of Ambient Intelligence and Humanized Computing*, pp. 1-17, 2020. [CrossRef] [Google Scholar] [Publisher Link]

[4] Carlos Van Mieghem, Marc Sabbe, and Daniel Knockaert, "The Clinical Value of the ECG in Non-Cardiac Conditions," *Chest*, vol. 125, no. 4, pp. 1561-1576, 2004. [CrossRef] [Google Scholar] [Publisher Link]

[5] Care I. E, "Part 8: Stabilization of the Patient with Acute Coronary Syndromes," *Circulation*, vol. 112, no. 24, pp. IV-90-IV-110, 2005. [CrossRef] [Google Scholar] [Publisher Link]

[6] Hongqiang Li et al., "Arrhythmia Classification Based on Multi-Domain Feature Extraction for an ECG Recognition System," *Sensors*, vol. 16, no. 10, 2016. [CrossRef] [Google Scholar] [Publisher Link]

[7] A. Pushpa, and I. Santi Prabha, "Implementation of Constrained Stability Least Mean Square Algorithm for Suppression of Noise in Cardiac Signals," *International Journal of Emerging Technology and Advanced Engineering*, vol. 3, no. 8, pp. 187-190, 2013. [Google Scholar] [Publisher Link]

[8] Ubedur Rehman, and V. S. Jadhav, "Noise Removal from ECG using Modified CSLMS Algorithm," *International Journal of Electronics, Communication and Instrumentation Engineering Research and Development*, vol. 4, no. 3, pp. 53-60, 2014. [Google Scholar] [Publisher Link]

[9] Madapuri Rudra Kumar, and Vinit Kumar Gunjan, "Review of Machine Learning Models for Credit Scoring Analysis," *Ingeniería Solidaria*, vol. 16, no. 1, pp. 1-16, 2020. [CrossRef] [Google Scholar] [Publisher Link]

[10] Anitha Boge, V. Vijaya, and K. Kishan Rao, "Clearing Artifacts using a Constrained Stability Least Mean Square Algorithm from Cardiac Signals," *International Journal of Scientific and Engineering Research*, vol. 3, no. 11, pp. 421-426, 2012. [Google Scholar] [Publisher Link]

[11] Joo-Chang Kim, and Kyungyong Chung, "Neural-Network Based Adaptive Context Prediction Model for Ambient Intelligence," *Journal of Ambient Intelligence and Humanized Computing*, vol. 11, no. 4, pp. 1451-1458, 2020. [CrossRef] [Google Scholar] [Publisher Link]

[12] Nusrat J. Shoumy et al., "Multimodal Big Data Affective Analytics: A Comprehensive Survey using Text, Audio, Visual and Physiological Signals," *Journal of Network and Computer Applications*, vol. 149, pp. 1-34, 2020. [CrossRef] [Google Scholar] [Publisher Link]

[13] João Rodrigues, David Belo, and Hugo Gamboa, "Noise Detection on ECG Based on Agglomerative Clustering of Morphological Features," *Computers in Biology and Medicine*, vol. 87, pp. 322-334, 2017. [CrossRef] [Google Scholar] [Publisher Link]

[14] Haemwaan Sivaraks, and Chotirat Ann Ratanamahatana, "Robust and Accurate Anomaly Detection in ECG Artifacts using Time Series Motif Discovery," *Computational and Mathematical Methods in Medicine*, vol. 2015, pp. 1-20, 2015. [CrossRef] [Google Scholar] [Publisher Link]

[15] Udit Satija, Barathram Ramkumar, and M. Sabarimalai Manikandan, "Automated ECG Noise Detection and Classification System for Unsupervised Healthcare Monitoring," *IEEE Journal of Biomedical and Health Informatics*, vol. 22, no. 3, pp. 722-732, 2018. [CrossRef] [Google Scholar] [Publisher Link]

[16] S. Cuomo et al., "A Revised Scheme for Real Time ECG Signal Denoising Based on Recursive Filtering," *Biomedical Signal Processing and Control*, vol. 27, pp. 134-144, 2016. [CrossRef] [Google Scholar] [Publisher Link]

[17] Santosh Kumar Yadav, Rohit Sinha, and Prabin Kumar Bora, "Electrocardiogram Signal Denoising using Non-Local Wavelet Transform Domain Filtering," *IET Signal Processing*, vol. 9, no. 1, pp. 88-96, 2015. [CrossRef] [Google Scholar] [Publisher Link]

[18] M. Izzetoglu et al., "Motion Artifact Cancellation in NIR Spectroscopy using Wiener Filtering," *IEEE Transactions on Biomedical Engineering*, vol. 52, no. 5, pp. 934-938, 2005. [CrossRef] [Google Scholar] [Publisher Link]

[19] Guohua Lu et al., "Removing ECG Noise from Surface EMG Signals using Adaptive Filtering," *Neuroscience Letters*, vol. 462, no. 1, pp. 14-19, 2009. [CrossRef] [Google Scholar] [Publisher Link]

[20] C. Marque et al., "Adaptive Filtering for ECG Rejection from Surface EMG Recordings," *Journal of Electromyography and Kinesiology*, vol. 15, no. 3, pp. 310-315, 2005. [CrossRef] [Google Scholar] [Publisher Link]

[21] Sarang L. Joshi, Rambabu A Vatti, and Rupali V. Tornekar, "A Survey on ECG Signal Denoising Techniques," *2013 International Conference on Communication Systems and Network Technologies*, pp. 60-64, 2013. [CrossRef] [Google Scholar] [Publisher Link]

[22] Brij N. Singh, and Arvind K. Tiwari, "Optimal Selection of Wavelet Basis Function Applied to ECG Signal Denoising," *Digital Signal Processing*, vol. 16, no. 3, pp. 275-287, 2006. [CrossRef] [Google Scholar] [Publisher Link]

[23] Md. Abdul Awal et al., "An Adaptive Level Dependent Wavelet Thresholding for ECG Denoising," *Biocybernetics and Biomedical Engineering*, vol. 34, no. 4, pp. 238-249, 2014. [CrossRef] [Google Scholar] [Publisher Link]

[24] S. Sandhya Kumari, and K. Sandhya Rani, "Selection of MSER Region Based Ultrasound Doppler Scan Image Big Data Classification using a Faster RCNN Network," *International Journal of Computer Engineering in Research Trends*, vol. 9, no. 10, pp. 184-192, 2022. [Publisher Link]

[25] Pratik Singh, Gayadhar Pradhan, and Shahnawazuddin S, "Denoising of ECG Signal by Non-Local Estimation of Approximation Coefficients in DWT," *Biocybernetics and Biomedical Engineering*, vol. 37, no. 3, pp. 599-610, 2017. [CrossRef] [Google Scholar] [Publisher Link]

[26] Manas Rakshit, and Susmita Das, "An Efficient ECG Denoising Methodology using Empirical Mode Decomposition and Adaptive Switching Mean Filter," *Biomedical Signal Processing and Control*, vol. 40, pp. 140-148, 2018. [CrossRef] [Google Scholar] [Publisher Link]

[27] Salim Lahmiri, "Comparative Study of ECG Signal Denoising by Wavelet Thresholding in Empirical and Variational Mode Decomposition Domains," *Healthcare Technology Letters*, vol. 1, no. 3, pp. 104-109, 2014. [CrossRef] [Google Scholar] [Publisher Link]

[28] Kandala N. V. P. S. Rajesh, and Ravindra Dhuli, "Classification of Imbalanced ECG Beats using Re-Sampling Techniques and AdaBoost Ensemble Classifier," *Biomedical Signal Processing and Control*, vol. 41, pp. 242-254, 2018. [CrossRef] [Google Scholar] [Publisher Link]

[29] Paweł Pławiak, and U. Rajendra Acharya, "Novel Deep Genetic Ensemble of Classifiers for Arrhythmia Detection using ECG Signals," *Neural Computing and Applications*, vol. 32, no. 15, pp. 11137-11161, 2020. [CrossRef] [Google Scholar] [Publisher Link]

[30] P. E. Tikkanen, "Nonlinear Wavelet and Wavelet Packet Denoising of Electrocardiogram Signal," *Biological Cybernetics*, vol. 80, no. 4, pp. 259-267, 1999. [CrossRef] [Google Scholar] [Publisher Link]

[31] Mangi Kang, Jaelim Ahn, and Kichun Lee, "Opinion Mining using Ensemble Text Hidden Markov Models for Text Classification," *Expert Systems with Applications*, vol. 94, pp. 218-227, 2018. [CrossRef] [Google Scholar] [Publisher Link]

[32] N. Sathya, "An Area Efficient Denoising Architecture using Adaptive Rank Order Filter," *International Journal of Recent Engineering Science (IJRES)*, vol. 1, no. 1, pp. 11-15, 2014. [Publisher Link]

[33] S. Iravanian, and L. Tung, "A Novel Algorithm for Cardiac Biosignal Filtering Based on Filtered Residue Method," *IEEE Transactions on Biomedical Engineering*, vol. 49, no. 11, pp. 1310-1317, 2002. [CrossRef] [Google Scholar] [Publisher Link]

[34] J. M. Leski, "Robust Weighted Averaging of Biomedical Signals," *IEEE Transactions on Biomedical Engineering*, vol. 49, no. 8, pp. 796-804, 2002. [CrossRef] [Google Scholar] [Publisher Link]

[35] Norden E. Huang et al., "The Empirical Mode Decomposition and the Hilbert Spectrum for Nonlinear and Non-Stationary Time Series Analysis," *Proceedings: Mathematical, Physical and Engineering Sciences*, vol. 454, no. 1971, pp. 903-995, 1998. [CrossRef] [Google Scholar] [Publisher Link]

[36] Md. Ashfanoor Kabir, and Celia Shahnaz, "Denoising of ECG Signals Based on Noise Reduction Algorithms in EMD and Wavelet Domains," *Biomedical Signal Processing and Control*, vol. 7, no. 5, pp. 481-489, 2012. [CrossRef] [Google Scholar] [Publisher Link]

[37] V. Kishen Ajay Kumar et al., "Dynamic Wavelength Scheduling by Multiobjective in OBS Networks," *Journal of Mathematics*, vol. 2022, 2022. [CrossRef] [Google Scholar] [Publisher Link]

[38] Allan Kardec Barros, Ali Mansour, and Noboru Ohnishi, "Removing Artifacts from Electrocardiographic Signals using Independent Components Analysis," *Neurocomputing*, vol. 22, no. 1-3, pp. 173-186, 1998. [CrossRef] [Google Scholar] [Publisher Link]

[39] S. Sandhya Kumari, and K. Sandhya Rani, "Empirical Mode Decomposition and Dual Sigmoid Activation Function-Based Faster RCNN for Big Data Doppler Scan Image Classification," *International Journal of Computer Engineering in Research Trends*, vol. 8, no. 9, pp. 151-165, 2021. [Google Scholar] [Publisher Link]

[40] Muhammad Zia Ur Rahman, Rafi Ahamed Shaik, and D. V. Rama Koti Reddy, "Efficient and Simplified Adaptive Noise Cancelers for ECG Sensor Based Remote Health Monitoring," *IEEE Sensors Journal*, vol. 12, no. 3, pp. 566-573, 2012. [CrossRef] [Google Scholar] [Publisher Link]

[41] M. M. Venkata Chalapathi et al., "Ensemble Learning by High-Dimensional Acoustic Features for Emotion Recognition from Speech Audio Signal," *Security and Communication Networks*, vol. 2022, 2022. [CrossRef] [Google Scholar] [Publisher Link]

[42] Dahee Chung et al., "Construction of an Electrocardiogram Database Including 12 Lead Waveforms," *Healthcare Informatics Research*, vol. 24, no. 3, pp. 242-246, 2018. [CrossRef] [Google Scholar] [Publisher Link]

[43] Angelina Prima Kurniati et al., "Process Mining in Oncology using the MIMIC-III Dataset," *Journal of Physics: Conference Series*, vol. 971, no. 1, 2018. [CrossRef] [Google Scholar] [Publisher Link]

[44] Dukyong Yoon et al., "System for Collecting Biosignal Data from Multiple Patient Monitoring Systems," *Healthcare Informatics Research*, vol. 23, no. 4, pp. 333-337, 2017. [CrossRef] [Google Scholar] [Publisher Link]

[45] Shailesh Kumar, Damodar Panigrahy, and P. K. Sahu, "Denoising of Electrocardiogram (ECG) Signal by using Empirical Mode Decomposition (EMD) with Non-Local Mean (NLM) Technique," *Biocybernetics and Biomedical Engineering*, vol. 38, no. 2, pp. 297-312, 2018. [CrossRef] [Google Scholar] [Publisher Link]

[46] Yunzheng Wang et al., "Recent Advances in Real-Time Spectrum Measurement of Soliton Dynamics by Dispersive Fourier Transformation," *Reports on Progress in Physics*, vol. 83, no. 11, 2020. [CrossRef] [Google Scholar] [Publisher Link]

[47] Gautier Marti et al., "A Review of Two Decades of Correlations, Hierarchies, Networks and Clustering in Financial Markets," *Progress in Information Geometry*, pp. 245-274, 2021. [CrossRef] [Google Scholar] [Publisher Link]

[48] Solomon Osarumwense Alile, "An Ischemic Heart Disease Prediction Model Based on Observed Symptoms using Machine Learning," *International Journal of Computer Engineering in Research Trends*, vol. 7, no. 9, pp. 9-22, 2020. [Google Scholar] [Publisher Link]

[49] Tae-Ki An, and Moon-Hyun Kim, "A New Diverse AdaBoost Classifier," *2010 International Conference on Artificial Intelligence and Computational Intelligence*, pp. 359-363, 2010. [CrossRef] [Google Scholar] [Publisher Link]

[50] Benedetto Barabino et al., "An Integrated Approach to Select Key Quality Indicators in Transit Services," *Social Indicators Research*, pp. 1-36, 2020. [CrossRef] [Google Scholar] [Publisher Link]

[51] S. Celin, and K. Vasanth, "ECG Signal Classification using Various Machine Learning Techniques," *Journal of Medical Systems*, vol. 42, no. 12, pp. 1-11, 2018. [CrossRef] [Google Scholar] [Publisher Link]

[52] G. B. Moody, and R. G. Mark, "The Impact of the MIT-BIH Arrhythmia Database," *IEEE Engineering in Medicine and Biology Magazine*, vol. 20, no. 3, pp. 45-50, 2001. [CrossRef] [Google Scholar] [Publisher Link]

[53] M. M. Venkata Chalapathi et al., "Ensemble Learning by High-Dimensional Acoustic Features for Emotion Recognition from Speech Audio Signal," *Security and Communication Networks*, vol. 2022, 2022. [CrossRef] [Google Scholar] [Publisher Link]

[54] T. S. Lugovaya, "*Biometric Human Identification Based on ECG*," Master's Thesis, Faculty of Computing Technologies and Informatics, Electrotechnical University, 2005. [Publisher Link]

[55] Raghavendra Badiger, and M. Prabhakar, "ASCNet-ECG: Deep Autoencoder Based Attention Aware Skip Connection Network for ECG Filtering," *International Journal of Engineering Trends and Technology*, vol. 71, no. 2, pp. 382-398, 2023. [CrossRef] [Google Scholar] [Publisher Link]

[56] Steven Smith, *Digital Signal Processing: A Practical Guide for Engineers and Scientists*, Newnes, An Imprint of Elsevier Science, 2013. [Google Scholar] [Publisher Link]

[57] Python (n.d.), [Online]. Available: https://www.python.org/

[58] V. R. S. Rajesh Kumar, and A. Sivanantharaja, "Feed Forward Neural Network Optimized using PSO and GSA for the Automatic Classification of Heartbeat," *Middle-East Journal of Scientific Research*, vol. 23, no. 5, pp. 896-901, 2015. [Google Scholar] [Publisher Link]

[59] S. Arivoli, "A Novel SVM Neural Network Based Clinical Diagnosis of Cardiac Rhythm," *SSRG International Journal of Medical Science*, vol. 4, no. 1, pp. 8-14, 2017. [CrossRef] [Google Scholar] [Publisher Link]

[60] C. Haritha, M. Ganesan, and E. P. Sumesh, "A Survey on Modern Trends in ECG Noise Removal Techniques," *2016 International Conference on Circuit, Power and Computing Technologies (ICCPCT)*, pp. 1-7, 2016. [CrossRef] [Google Scholar] [Publisher Link]

[61] R. S. Khandpur, *Handbook of Biomedical Instrumentation*, McGraw Hill Education (India) Private Limited, 3rd Ed., 2014. [Google Scholar] [Publisher Link]

[62] P. K. Dash, "Electrocardiogram Monitoring," *Indian Journal of Anaesthesia*, vol. 46, no. 4, pp. 251-260, 2002. [Google Scholar] [Publisher Link]